Science Advances
AAAS

advances.sciencemag.org/cgi/content/full/5/10/eaax6550/DC1

Supplementary Materials for

Nontrivial quantum oscillation geometric phase shift in a trivial band

Biswajit Datta*, Pratap Chandra Adak, Li-kun Shi, Kenji Watanabe, Takashi Taniguchi, Justin C. W. Song*, Mandar M. Deshmukh*

*Corresponding author. Email: deshmukh@tifr.res.in (M.M.D.); biswajitdattaju69@gmail.com (B.D.); justinsong@ntu.edu.sg (J.C.W.S.)

Published 18 October 2019, *Sci. Adv.* **5**, eaax6550 (2019)
DOI: 10.1126/sciadv.aax6550

This PDF file includes:

Section S1. Device fabrication

We use the Polypropylene carbonate (PPC) polymer based dry method to make the hBN-trilayer graphene-hBN stack (*43*). E-beam lithography is used to design the electrodes. Argon-Oxygen (1:1 ratio) plasma etching is used to define the one-dimensional electrical contacts followed by the metal deposition (3 nm Chromium, 15 nm Palladium, 30 nm Gold) (*44*). To design a top gate we transfer one more layer of hBN as the gate insulator. The final step of e-beam lithography is done to design the metal top gate. Fig. S1 shows the optical micrograph of two devices. Dimension of device - A is 9.5 µm × 7.5 µm and the mobility near the density of our interest is ∼500,000 $cm^2V^{-1}s^{-1}$. We show all the data in the main manuscript from device - A. Data from device - B is shown in Supplementary Materials V.

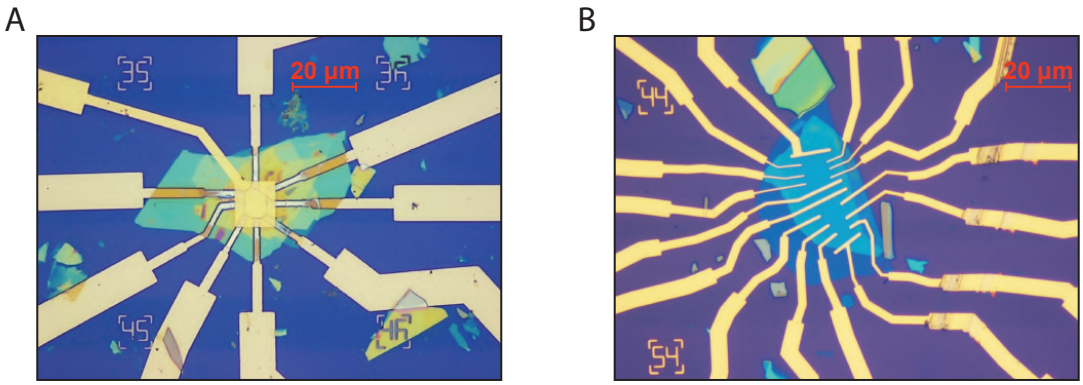

Fig. S1. Optical micrograph of devices.(A) Optical micrograph of an ABA-trilayer graphene device (device - A). The graphene is encapsulated by two layers of hBN. An additional hBN (for top gate insulator) was transferred on the completed device to make a uniform top gate. (B) Optical micrograph of another ABA-trilayer graphene device (device - B).

Section S2. Determination of the BLG-like LL index from the experimental Hall conductance

Following the previous theoretical study (*32*), we numerically calculate the LL energy diagram shown in fig. S2a. We consider the full tight binding Hamiltonian of ABA-trilayer graphene (*32*) with all the hopping parameters. Below are the band parameters we have used for all calculations: γ_0=3.1 eV, γ_1=390 meV, γ_2=-20 meV, γ_3=315 meV, γ_4=120 meV,

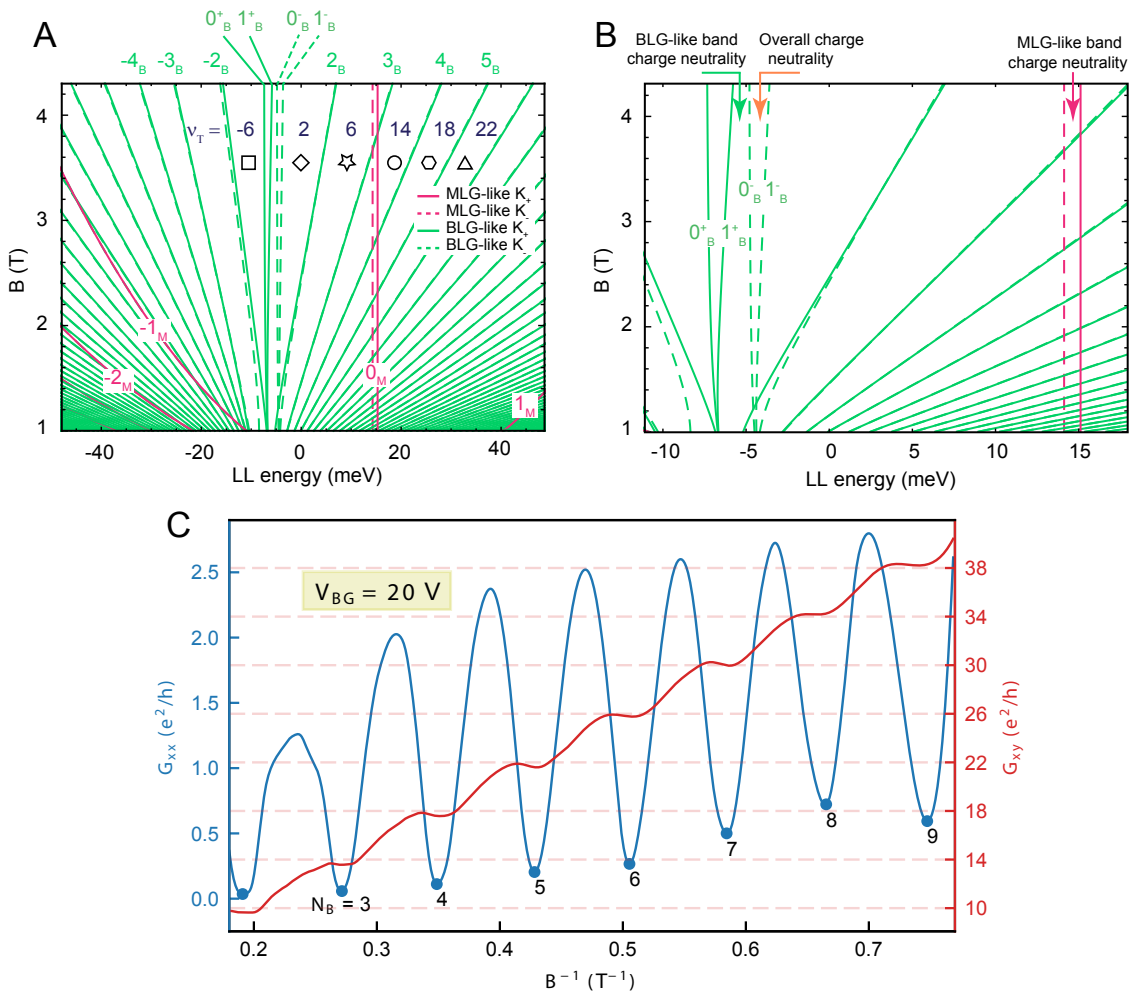

Fig. S2. Calculation of the BLG-like LL index from the total filling factor. (A) Different regions in the LL diagram are marked for which we show the calculation of the LL index. (B) Zoomed-in LL diagram showing the charge neutrality points of the MLG-like bands, BLG-like bands and the overall charge neutrality point of the system. Band specific filling factors are counted from their band specific charge neutrality points whereas the total filling factor is counted from the overall charge neutrality point. (C) Experimentally measured G_{xx} and G_{xy} as a function of the magnetic field on the electron side. LL indices at all the minima are marked and are given by $N_B=\frac{1}{4}(\nu_T-2)$.

γ_5=18 meV, δ=20 meV, Δ_2=4.3 meV which were calculated by matching the experimental LL crossing points with theory. The details of the band parameters' determination and details of the numerical calculation are described in our earlier study (*39*).

Fig. S2a shows that the MLG-like and BLG-like LL origins are shifted. We note that overall charge neutrality of the system is located in between 0_B and 1_B electron-like LLs

(fig. S2b) where Hall conductance goes to zero. Total filling factor (counted from the overall charge neutrality point) can be written as the sum of MLG-like filling factor (ν_M) counted from the MLG-like band origin and BLG-like filling factor (ν_B) counted from the BLG-like band origin: $\nu_T=\nu_M+\nu_B$. If N_M is the LL index of the MLG-like LLs then filling factor of the MLG-like band above and below the band gap is given by $\nu_M=4(N_M\pm0.5)$. Similarly, if N_B is the LL index of the BLG-like LLs then filling factor of the BLG-like band (for $N_B > 0$) is given by $\nu_B=4N_B$. We find the total filling factor (ν_T) from the experimentally measured quantized Hall conductance (G_{xy}) data. Fig. S2c shows a line slice of the G_{xx} and G_{xy} as a function of the magnetic field at V_{BG}=20 V on the electron side. Total filling factor is given by the integers where the quantum Hall G_{xy} plateaus occur. Filling factor of the MLG-like band (ν_M) can also be easily counted from the experimental fan diagram since the MLG-like LLs are very sparse and have a distinct parabolic dispersion. This allows us to calculate $N_B=\frac{1}{4}(\nu_T-\nu_M)$. Table S1 shows the calculated BLG-like LL indices at different filling factors marked in fig. S2a.

Table S1. Extracted LL index at 4 T for different filling factors.

Below the MLG-like band gap					
Symbol	ν_T	$\nu_M=4(N_M-0.5)$	$\nu_B=4N_B$	N_M	N_B
□	-6	-2	-4	0	-1
◇	2	-2	4	0	1
★	6	-2	8	0	2
Above the MLG-like band gap					
Symbol	ν_T	$\nu_M=4(N_M+0.5)$	$\nu_B=4N_B$	N_M	N_B
○	14	2	12	0	3
⬡	18	2	16	0	4
△	22	2	20	0	5

Section S3. Determination of the phase from the simulated density of states (DOS)

A. Fitting the DOS oscillation at a constant energy

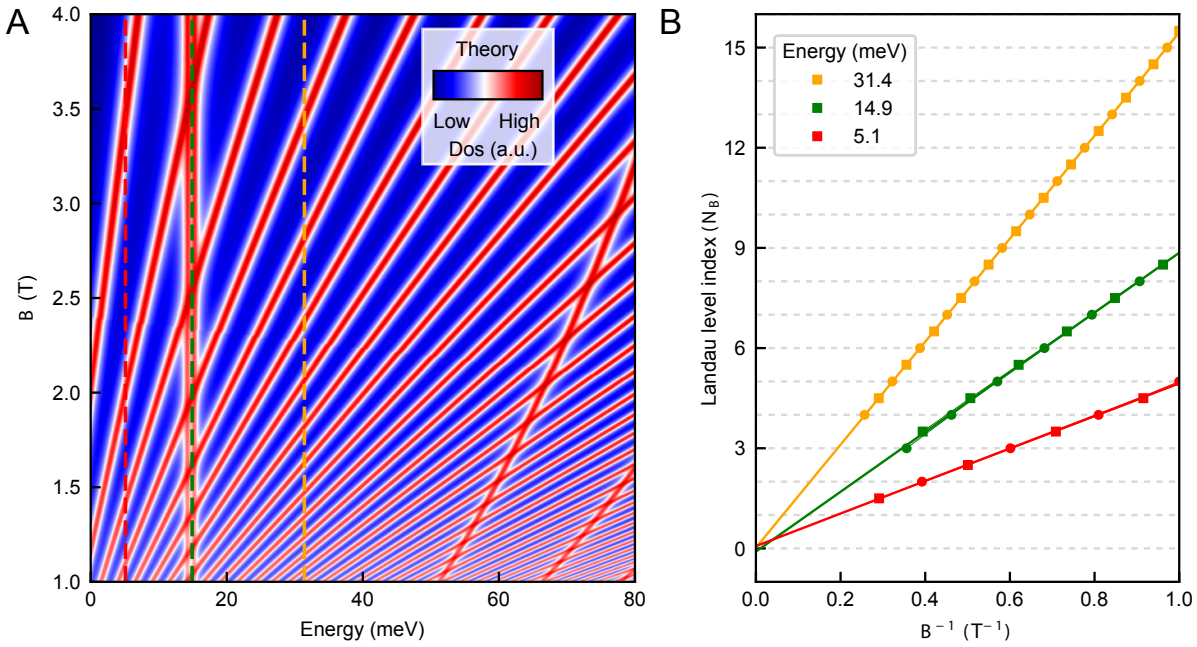

Fig. S3. Fitting using the DOS oscillations at a constant energy. (A) Calculated DOS as a function of energy and magnetic field. (b) BLG-like LL Fits below the band gap (red), in the band gap (green) and above the band gap (yellow).

We extract Berry's phase also by fitting the theoretical DOS oscillations (*39*). Fig. S3a shows the DOS as a function of Fermi energy and magnetic field. BLG-like DOS oscillation extrema are fitted at a line of constant energy. Like the experiment, integer (half-integer) LL indices are assigned at the minima (maxima) of the DOS oscillations. We note that the DOS maxima positions correspond to the experimental G_{xx} maxima. All the fits (for the Fermi level below the MLG-like band gap, in the MLG-like band gap and above the MLG-like band gap) show zero intercepts – irrespective of the Fermi level position in the MLG-like band (see fig. S3b). This shows that the BLG-like band individually retains its 2π Berry's phase.

B. Fitting the DOS oscillation at a constant density

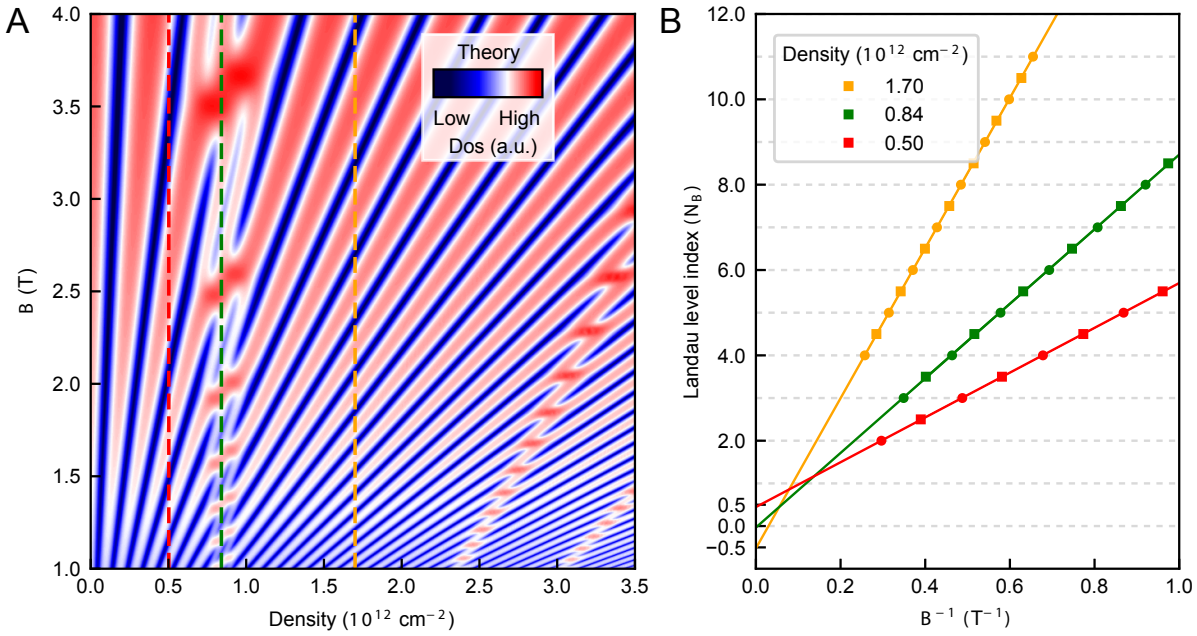

Fig. S4. Fitting using the DOS oscillations at a constant density. (A) Calculated DOS as a function of density and magnetic field. (B) BLG-like LL Fits below the band gap (red), in the band gap (green) and above the band gap (yellow).

We carry out similar LL fits as shown in the main manuscript using the theoretically calculated DOS oscillations (*39*) (fig. S4a) in the density magnetic field space. Like in the experiment, BLG-like DOS oscillation extrema are fitted at a line of constant density. We see similar anomalous phase: π below the MLG-like band gap and -π above the MLG-like band gap while it goes to zero in the MLG-like band gap (fig. S4b). As we have explained in the manuscript, this additional phase picked up by the trivial BLG-like Fermi surface is because of the constraint on the total density in a multiband system. This constraint naturally occurs because experimentally the SdH oscillations are measured at a constant total density controlled by the gate voltage. The comparison between the fits done at a constant energy (fig. S3b) and at a constant density (fig. S4b) clearly shows the role of density constraint to determine the phase of the quantum oscillations in a multiband system.

Section S4. Determination of the phase of the BLG-like SdH oscillations when multiple MLG-like LLs are filled

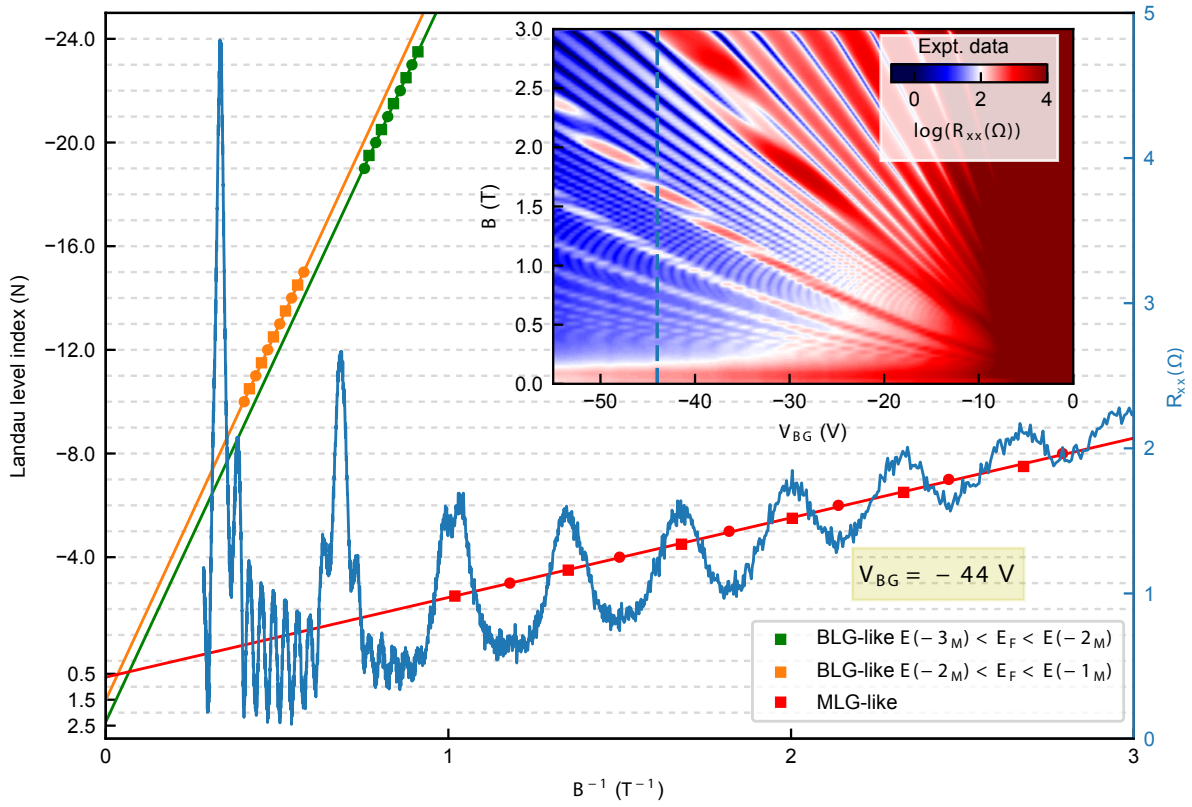

Fig. S5. Extracting the phase and SdH frequency when multiple MLG-like LLs are filled. The red line is a fit of the MLG-like LLs when the BLG-like LLs are not resolved. Orange and green lines are the fit of BLG-like LLs for which the Fermi energy is at -1_{M} and -2_{M} completely filled MLG-like LLs respectively. Slope of the MLG-like LL fit is almost 10 times smaller than the slope of the BLG-like LL fits because the BLG-like Fermi surface area is almost 10 times larger than the MLG-like Fermi surface area for this Fermi energy. The inset shows the color plot of the resistance on the hole side. The overlaid blue dashed line shows the position of the plotted SdH oscillation at V_{BG}=-44 V.

In general, the SdH oscillations have contributions from both the bands: $\Delta G_{\mathrm{xx}} = G_{\mathrm{M}} \cos[2\pi(\frac{B_{\mathrm{FM}}}{B} + \gamma_{\mathrm{M}})] + G_{\mathrm{B}} \cos[2\pi(\frac{B_{\mathrm{FB}}}{B} + \gamma_{\mathrm{B}})]$. Since the first few MLG-like LLs have large gaps, it is possible that two successive MLG-like LLs contain several BLG-like LL oscillations. We fit such BLG-like LL oscillations contained between two successive MLG-like LLs away from the crossing regions. When the Fermi energy goes through the BLG-like LL oscillations in between N_{M} and $(N+1)_{\mathrm{M}}$ LLs, the MLG-like filling factor remains constant

to $\nu_{\rm M} = 4(N_{\rm M} \pm 0.5)$ because of being in the LL gap of the MLG-like LLs . Following the arguments presented in the main text for this range of Fermi energy the SdH oscillations can be captured by

$$\Delta G_{\rm xx} = G_{\rm B} \cos[2\pi(\frac{B_{\rm FT}}{B} + \gamma_B - \frac{\nu_{\rm M}}{4})] \tag{S1}$$

In the main manuscript, we have shown the LL fits where only the lowest MLG-like LL is filled ($\nu_{\rm M} = \pm 2$). But, in general, the intercept of the BLG-like LL fitting depends on how many MLG-like LLs are filled.

If N and $\rm B_N$ are the LL index of the BLG-like LLs and the corresponding magnetic field at an SdH oscillation minima, then the equation of the fitting line is given by $N = \frac{B_{\rm FT}}{B_{\rm N}} + \frac{\Phi_{\rm B}}{2\pi}$ - $\frac{\nu_{\rm M}}{4}$. Here the slope $B_{\rm FT}$ relates to the total density ($\rm n_T$=$\frac{4e}{h} \times B_{\rm FT}$) and the total Fermi surface area ($\rm S_{FT}$=$\frac{2\pi e}{\hbar} \times B_{\rm FT}$). Now, only $\rm N_M$=0 and $\rm N_M$= -1 hole like LLs are filled, when the Fermi energy lies below the MLG-like band gap between the -$1_{\rm M}$ and -$2_{\rm M}$ LLs i.e. E(-$2_{\rm M}$) $< E_{\rm F} < E(-1_{\rm M})$. In this case the filling factor of the MLG-like band remains pinned to -6 making the equation of the fitting line $N = \frac{B_{\rm FT}}{B_{\rm N}} + \frac{\Phi_{\rm B}}{2\pi} + \frac{3}{2}$. Since, Berry's phase $\Phi_{\rm B}$=0 for BLG-like LLs, this returns 1.5 intercept at 1/B=0 (see the orange line in fig. S5). Similarly, $\rm N_M$=0, $\rm N_M$= -1 and $\rm N_M$= -2 hole like LLs are filled, when the Fermi energy lies below the MLG-like band gap between the -$2_{\rm M}$ and -$3_{\rm M}$ LLs i.e. E(-$3_{\rm M}$) $< E_{\rm F} < E(-2_{\rm M})$. In this case the filling factor of the MLG-like band remains pinned to -10 making the equation of the fitting line $N = \frac{B_{\rm FT}}{B_{\rm N}} + \frac{\Phi_{\rm B}}{2\pi} + \frac{5}{2}$. This results in 2.5 intercept at 1/B=0 (see the green line in fig. S5).

We also fit the MLG-like LLs at the low field when the BLG-like LLs are not resolved. At very low magnetic field $B < 1$ T (i.e. 1<1/B<3 in fig. S5), we resolve only MLG-like LLs since the LL spacing of the MLG-like bands are significantly larger than the BLG-like LLs. In this regime, the amplitude of the BLG-like SdH oscillations dies almost to zero, so, the SdH oscillation can be captured only in terms of the MLG-like LLs:

$$\Delta G_{\rm xx} = G_{\rm M} \cos[2\pi(\frac{B_{\rm FM}}{B} + \gamma_M)]. \tag{S2}$$

If N and $\rm B_N$ are the LL index of the MLG-like LLs and the corresponding magnetic field, then the equation of the fitting line is given by $N = \frac{B_{\rm FM}}{B_{\rm N}} + \frac{\Phi_{\rm M}}{2\pi}$. Here the slope $B_{\rm FM}$ relates to the MLG-like band density ($\rm n_M$=$\frac{4e}{h} \times B_{\rm FM}$) and the MLG-like Fermi surface area ($\rm S_{FM}$=$\frac{2\pi e}{\hbar} \times B_{\rm FM}$). Since, Berry's phase $\Phi_{\rm M}$=π for MLG-like LLs, this returns 0.5 intercept at 1/B=0. The red line in fig. S5 shows that indeed the intercept of the MLG-like LLs is

close to 0.5 confirming the nontrivial π Berry's phase. This again confirms that the MLG-like band individually retains its π Berry's phase and there is no hybridization between the bands. We note that the slope of the red line is almost an order of magnitude smaller than the orange and the green lines. This is because the Fermi surface area of the MLG-like band is roughly an order of magnitude smaller than the BLG-like Fermi surface area for this Fermi energy.

Section S5. Determination of the phase of the BLG-like SdH oscillations from another device

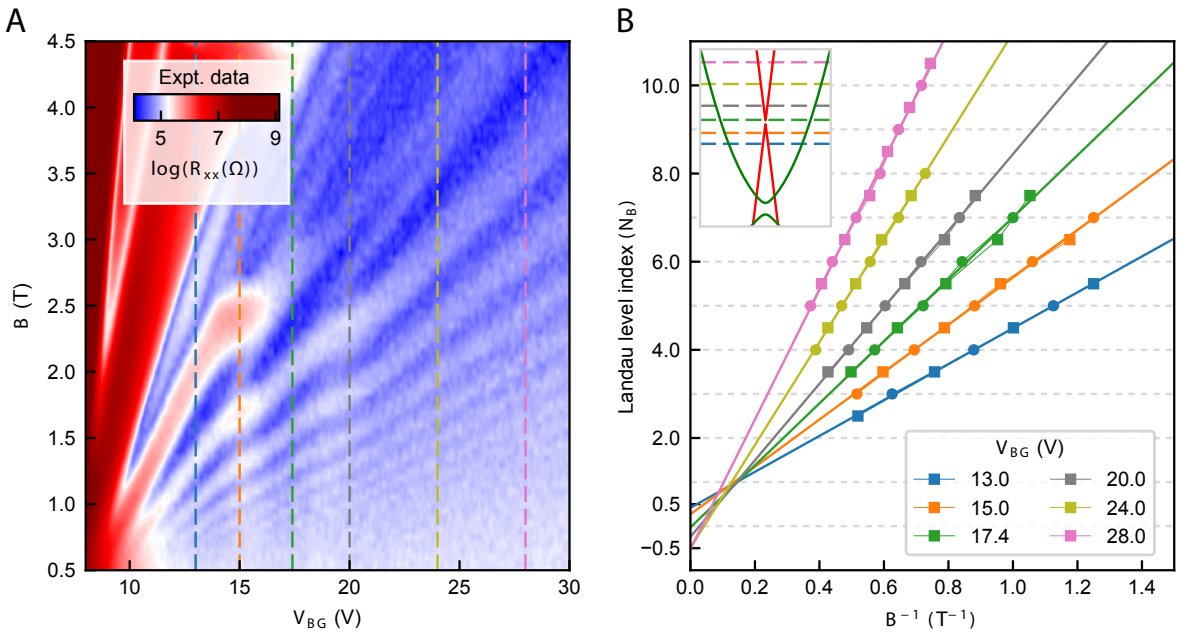

Fig. S6. Determination of the phase of the BLG-like SdH oscillations from another device. (A) Experimentally measured Landau level fan diagram from device - B. (B) LL index plot for the BLG-like SdH oscillations at different densities across the Dirac band gap. Gate voltage for all the fittings are marked with dashed lines of the corresponding color in the fan diagram (Panel-A).

Here we show the quantum oscillation phase analysis from device - B. Fig. S6a shows the experimentally measured Landau level fan diagram. We have observed similar phase variation of the BLG-like SdH oscillations across the MLG-like Dirac band gap (fig. S6b).

Section S6. Effect of electric field

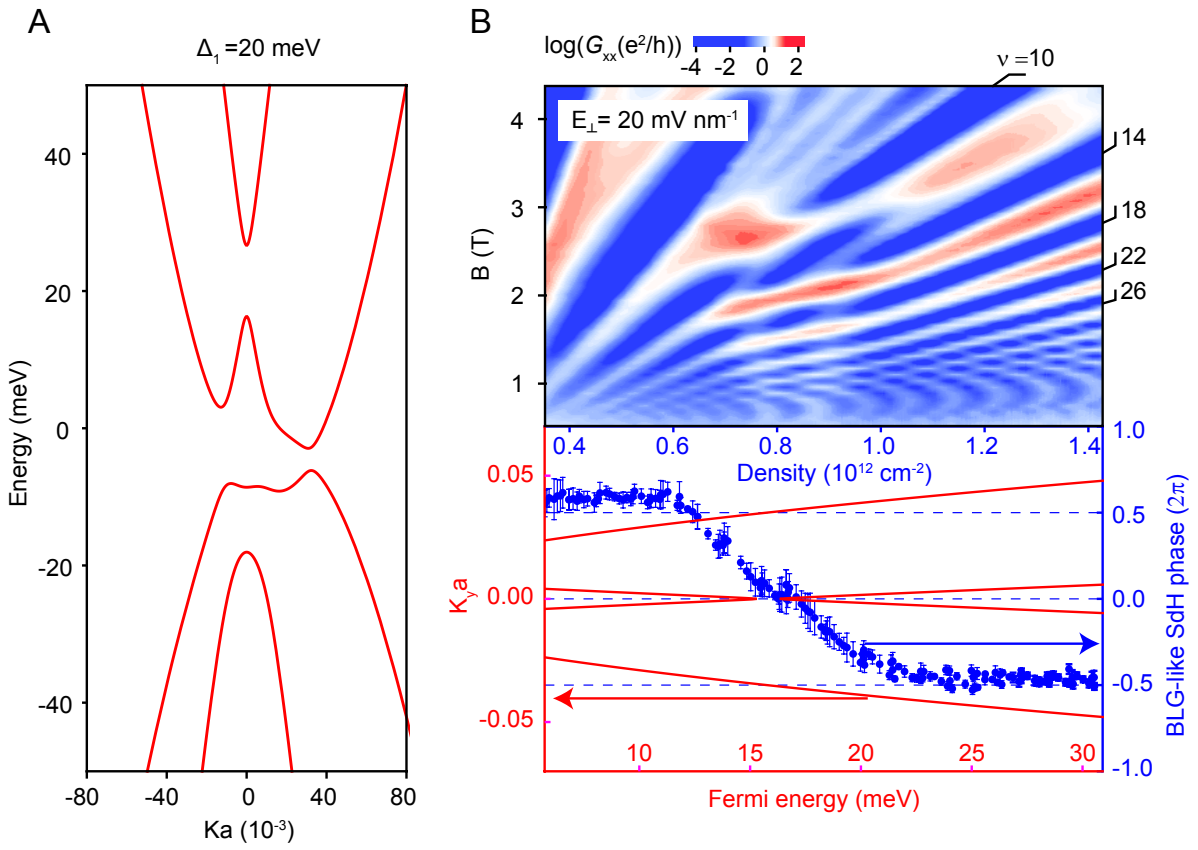

Fig. S7. Variation of the BLG-like SdH phase with Fermi energy at an electric field. (A) Hybridization of the bands due to an electric field (Δ_1 = 20 meV). Electric field increases the band gap between the Dirac cones from ∼1 meV to ∼10 meV. (B) Top panel: LL fan diagram as a function of magnetic field and density at at a small electric field (20 mV nm^{-1}). Bottom panel: measured phase as a function of density which shows a continuous variation around the MLG-like band gap (coloured blue). Theoretically calculated band diagram (coloured red) is overlaid on it.

Electric field is an interesting knob in multi-layer graphene. In the case of ABA-trilayer graphene, the hybridization between the linear and the quadratic bands depends on the electric field. So, at a high electric field, the two bands get hybridized significantly near the crossing points resulting in new bands which have mixed character – this regime is out of the scope of our study. However, our analysis focuses away from the MLG-like and the BLG-like band crossings – we focus near the Dirac band gap. At a low electric field, here, the effect of

the electric field is primarily to change the band gap between the Dirac cones (see fig. S7a). So, even at a finite electric field, the change of BLG-like SdH oscillation phase across the Dirac cone gap remains similar to the data phase variation at the zero electric field. We have analyzed our experimental data taken at a small electric field (20 mV nm^{-1}) which shows that the phase variation of the BLG-like SdH oscillations across the MLG-like band gap resembles closely with the data taken at a zero electric field (see fig. S7b).